Separation of Elastic and Plastic Timescales in a Phase Field Crystal Model

Audun Skaugen, Luiza Angheluta, and Jorge Viñals

Separation of elastic and plastic time scales in a phase field crystal model

Audun Skaugen* and Luiza Angheluta

Njord Center, Department of Physics, University of Oslo, P.O. 1048 Blindern, 0316 Oslo, Norway

Jorge Viñals

School of Physics and Astronomy, University of Minnesota,
116 Church St. SE, Minneapolis, MN 55455, USA

(Dated: November 16, 2018)

A consistent, small-scale description of plasticity and dislocation motion in a crystalline solid is presented based on the phase field crystal description. By allowing for independent mass motion and lattice distortion, the crystal can maintain elastic equilibrium on the timescale of plastic motion. We show that the singular (incompatible) strains are determined by the phase field crystal density, while the smooth distortions are constrained to satisfy elastic equilibrium. A numerical implementation of the model is presented, and used to study a benchmark problem: the motion of an edge dislocation dipole in a triangular lattice. The time dependence of the dipole separation agrees with continuum elasticity with no adjustable parameters.

The plasticity of small-scale crystals under load is characterized by intermittent strain bursts and dislocation avalanches [1–7]. This complex response with scale-free fluctuations lies squarely outside of classical continuum plasticity theory, which assumes coarse-grained volumes containing many defects, and hence valid on macroscopic scales. More recent continuum plasticity theories [8–17] are developed at nanoscale, as new state-of-art experiments provide high-resolution imaging of crystal defects and their evolution [18–20]. These theoretical developments focus however on the individual dislocation motion rather their collective effects and the scale-free phenomena in crystal plasticity. Analogies with nonequilibrium critical phenomena, like depinning transition [21] and jamming transition [5], have been proposed yet not convincingly. Some statistical properties of interacting lattice defects can be reproduced by discrete dislocation dynamics models [4], which have arbitrary parameters controlling the dislocation mobility and kinetics. We therefore lack a consistent theoretical description of collective dislocation dynamics without ad-hoc parameters.

The Phase Field Crystal model (PFC) is a leading contender for the efficient mesoscale modelling of crystallization phenomena [9, 22] and dislocation motion [6, 23–25]. With a diffusive evolution of the PFC density field, the existing PFC formulations are not adequate models of small-scale crystal plasticity, when lacking a consistent separation of timescales between the fast relaxation of the elastic (smooth) distortions and the slow dynamics of crystal defects associated to singular distortions. This was recognized early and resolved by phenomenologically adding ballistic degrees of freedom propagating the fast elastic perturbations [23], which is some particu-

lar limit of a hydrodynamic description for colloidal crystals. More recent studies use the mode expansion of the PFC density field to impose constraints on the phase evolution of the periodic modes to ensure elastic equilibrium [26, 27]. This description works for a perfect "soft" crystal near the critical point, and may not generalize nicely to defected crystals far away from the melting point.

In this letter, we propose a consistent way of implementing the timescale separation by introducing an independent variable related to static elastic distortions. The elastostatic condition is added to the diffusive evolution of the PFC density field which, as we have recently shown [25], is an order parameter for the topological defects as sources of singular distortions and their dissipative dynamics. As a classic example, the relative glide motion of two edge dislocations of opposite Burger's vectors under each other's stress field is studied in a triangular lattice. In contrast with a direct solution of the purely diffusive PFC model, we recover the internal stress fields and dislocation velocities consistent with elasticity theory. Our method bridges nicely between atomistic and continuum formulations. It is applicable to both two (2D) and three (3D) dimensional matter, different crystal symmetries and a variable quenching depth range, thus being a suitable model to quantitatively study complex phenomena in small-scale crystal plasticity with minimum input parameters.

A continuum theory of plasticity starts from the statement of incompatibility of the deformation gradient tensor

$$\epsilon_{ilm}\partial_l w_{mk} = \alpha_{ik}, \quad w_{mk} = \partial_m u_k \quad (1)$$

where ϵ_{ilm} is the anti symmetric Levi-Civita tensor, α_{ik} the dislocation density tensor, and w_{mk} the distortion tensor [28, 29] associated with the deformation field u_k. The integral of α_{ik} over a surface is the sum of the

Burger's vectors $\mathbf{b}$ corresponding to all the n dislocation lines that pierce the surface $\int_S \alpha_{ij} dS_j = \sum_n b_i^n$. For a given distribution of topological defects, α is fixed, but not the distortion w. This can be decomposed into a singular part, the curl of which yields α_{ij}, and a smooth strain which we denote by u_{ij}^δ. The smooth strain is compatible, $\epsilon_{ikm}\epsilon_{jln}\partial_{kl}u_{mn}^\delta = 0$. Regardless of the state of distortion, plastic motion is slow on the scale of lattice vibration, and occurs in mechanical equilibrium, as the stress σ_{ij} adiabatically follows the instantaneous distribution of dislocations, $\partial_j \sigma_{ij} = 0$. Closure generally requires a constitutive relation involving the stress and the smooth deformation. These considerations and appropriate boundary conditions are sufficient to specify the static problem. Dynamically, over the time scale appropriate for plastic flow, an evolution equation needs to be introduced for the dislocation density tensor [8, 10, 13, 30, 31]. In field dislocation dynamics theories, its evolution is kinematically related to the velocity of the dislocation lines, which in turn requires a constitutive definition in terms of a local free energy and a dissipation function [32]. The PFC model of defect motion, as currently formulated [9, 12, 27, 33], can be used to specify most of the static and dynamic features just described, but not all, as discussed below.

The PFC density $\psi(\mathbf{r}, t)$ is a physical order parameter that describes the dimensionless mass density of the crystalline phase and inherits the lattice periodicity, $\psi(\mathbf{r}) = \psi_0 + \sum_\mathbf{g} A_\mathbf{g} e^{i\mathbf{g}\cdot\mathbf{r}}$, where the sum extends over all reciprocal lattice vectors $\mathbf{g}$ of the lattice, and $A_\mathbf{g}$ are the complex amplitudes for each period mode. A non-convex free energy functional for an isothermal system $\mathcal{F}$ is introduced so that its minimizer ψ^* has the desired symmetry of the crystalline phase. Lattice constants appear as parameters. In dimensionless units, we use $\mathcal{F}[\psi] = \int d\mathbf{r} f(\psi, \nabla^2 \psi)$ with $f(\psi, \nabla^2\psi) = (\mathcal{L}\psi)^2/2 + r^2\psi^2/2 + \psi^4/4$, and $\mathcal{L} = 1+\nabla^2$ [9, 14, 34]. The only remaining constant parameter r is the dimensionless distance away from the symmetry breaking bifurcation. For $r > 0$, $\psi^* = 0$ is the only stable solution. For $r < 0$, and depending on the conserved spatial average ψ_0, ψ^* is periodic with wavenumber unity in our dimensionless units, but of various symmetries. For simplicity, we consider a 2D system where the equilibrium configuration is a triangular phase with lattice constant $a = 4\pi/\sqrt{3}$. The Burger's vector density in 2D is $B_k(\mathbf{r}) = \alpha_{3,k}(\mathbf{r}), k = 1, 2$. Our results, however, can be readily extended to 3D. The temporal evolution of the PFC density ψ is diffusive and given by

$$\partial_t \psi(\mathbf{r}, t) = \nabla^2 \frac{\delta \mathcal{F}}{\delta \psi(\mathbf{r}, t)} \tag{2}$$

where $\delta/\delta\psi(\mathbf{r}, t)$ stands for the variational derivative with respect to ψ.

For smooth distortions of ψ^*, the free energy $\mathcal{F}$ suffices to determine the stress-strain relation [12]. For small distortions, we define a non-singular stress σ^ψ [25]

$$\sigma_{ij}^\psi = \left\langle \tilde{\sigma}_{ij}^\psi \right\rangle_c, \quad \tilde{\sigma}_{ij}^\psi = [\partial_i \mathcal{L}\psi]\,\partial_j \psi - [\mathcal{L}\psi]\,\partial_{ij}\psi + f\delta_{ij}, \tag{3}$$

with the microscopic stress $\tilde{\sigma}_{ij}^\psi$ given by the local variation of $\mathcal{F}$ with $\partial_i u_j$, and $\langle \cdot \rangle_c$ denoting a spatial coarse-graining by convoluting the microscpic stress with a Gaussian with a width equal to a unit cell. σ_{ij}^ψ is symmetric and related to the strain field $u_{ij} = (\partial_i u_j + \partial_j u_i)/2$ according to linear elasticity. For the triangular phase under discussion, the relation is that of isotropic elasticity

$$\sigma_{ij}^\psi = \lambda \delta_{ij} u_{kk} + 2\mu u_{ij} \tag{4}$$

with Lamé coefficients $\lambda = \mu = 3A_0^2$ [25]. The quantity A_0 is the amplitude of the uniform mode in a multiple scale amplitude expansion of ψ^*.

Following early work on dislocation motion and grain boundaries in roll patterns [35, 36], the PFC theory has been used to study dislocation [13, 33] and grain boundary motion [37, 38]. Strain fields have been explicitly extracted [39], or imposed to analyze strained film epitaxy [40], and considered as the limiting case of phonon degrees of freedom [27]. More complex properties of defect motion such as specification of slip systems, defect mobilities, and Peierls barriers are also given by PFC dynamics [25, 41, 42] thus opening the door to the study of defect pinning, bursts, and avalanches. However, while elastic equilibrium states with a fixed defected configuration can be found given appropriate boundary conditions, any nonequilibrium local deformation of $\psi(\mathbf{r}, t)$ propagates only diffusively according to Eq. (2). The relevant transverse diffusion constant is small, and can even vanish [43]. This is not physical for a crystalline solid, as has been already recognized [23, 26, 27, 33]. In ordinary crystals, unlike PFC model, elastic equilibrium compatible with a transient distribution $\alpha_{ik}(\mathbf{r}, t)$ and boundary conditions is established quickly, in a time scale determined by damping of elastic waves in the medium.

To overcome this difficulty, we propose to use the PFC density $\psi(\mathbf{r}, t)$ only as an indicator function of defect location and topology, as well as governing local relaxation near defect cores. The PFC field $\psi(\mathbf{r}, t)$ determines the source for lattice incompatibility in Eq. (1), the solution of which is only a *particular singular solution* for the deformation field. A smooth distortion $\mathbf{u}^\delta$ (in the null space of the curl) must be added to this particular solution to enforce elastic equilibrium. At each time, $\psi(\mathbf{r}, t)$ obtained from Eq. (2) is then distorted $\psi'(\mathbf{r} + \mathbf{u}^\delta) = \psi(\mathbf{r})$ to ensure elastic equilibrium. This leads to a defect motion consistent with the Peach-Koehler force [25]. Plastic motion is uniquely specified, with the only constitutive input being the free energy functional $\mathcal{F}$. We discuss in what follows the details of our computational implementation, and specifically address the relative motion of a dislocation dipole in a 2D triangular phase.
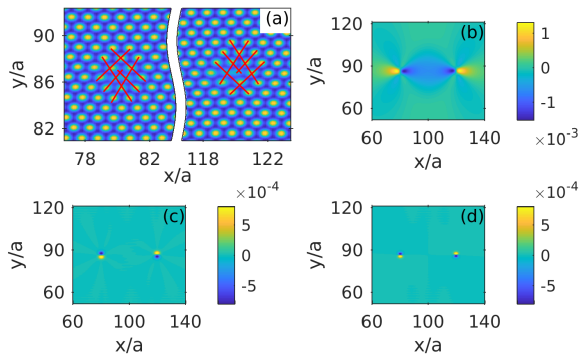
FIG. 1: (a): PFC ψ for an initial condition of two dislocations with opposite Burger's vectors on the same glide plane. Crystal planes in the $[11]$ and $[\bar{1}1]$ directions are indicated to illustrate the structure of the dislocations in the triangular lattice. (b): Coarse-grained shear stress σ_{xy}^{ψ}. (c): rhs of Eq. (8), divided by 2μ, showing dipolar sources at the dislocation positions. (d): Curl of the Burger's vector density as computed by demodulation in ref. [25], showing excellent agreement with (c).

For obtaining $\mathbf{u}^{\delta}$ at a given time t, we decompose the stress field into a singular part σ^{ψ} arising from $\psi(\mathbf{r}, t)$, and a small contribution σ^{δ} arising from the smooth distortion, so that $\sigma = \sigma^{\psi} + \sigma^{\delta}$ is in mechanical equilibrium $\nabla \cdot \sigma = 0$. This condition is satisfied by introducing the Airy function χ, which in 2D reads $\sigma_{ij} = \epsilon_{ik}\epsilon_{jl}\partial_{kl}\chi$. Inverting Eq. (4), we have in 2D

$$u_{ij} = \frac{1}{2}(\partial_i u_j + \partial_j u_i) = \frac{1}{2\mu}\left(\sigma_{ij} - \kappa\delta_{ij}\sigma_{kk}\right), \quad (5)$$

where $\kappa = \frac{\lambda}{2(\lambda+\mu)}$. Inserting Eq. (5) into the incompatibility relation in 2D $\epsilon_{ik}\epsilon_{jl}\partial_{kl}u_{ij} = \epsilon_{ij}\partial_i B_j(\mathbf{r})$ (e.g. [28]) and expressing the stress in terms of χ-function, we obtain that

$$\frac{1-\kappa}{2\mu}\nabla^4\chi = \epsilon_{ij}\partial_i B_j(\mathbf{r}), \quad (6)$$

where $B_j(\mathbf{r}) = \sum_\alpha b_j^n \delta(\mathbf{r} - \mathbf{r}_n)$ is the dislocation density in 2D for a configuration of dislocations with Burgers vector $\mathbf{b}^n$ at locations $\mathbf{r}_n$. In Ref. [25], we explicitly computed $\mathbf{B}(\mathbf{r})$ through complex demodulation of $\psi(\mathbf{r}, t)$. Demodulation yields both the amplitude and phase of the deformation field; the former going to zero at the defect core, the latter undergoing a discontinuity across a line that terminates at the core. Figure 1(a) shows a dislocation dipole in a 2D triangular lattice, and Figure 1(d) the right hand side of Eq. (6)) obtained by demodulation. We proceed differently here and introduce a more efficient numerical procedure that does not require demodulation. The smooth strain u_{ij}^{δ} is compatible ($\epsilon_{ik}\epsilon_{jl}\partial_{ij}u_{kl}^{\delta} = 0$) and therefore, with Eq. (5), the corresponding stress satisfies,

$$\epsilon_{ik}\epsilon_{jl}\partial_{ij}\left(\sigma_{kl}^{\delta} - \kappa\delta_{kl}\sigma_{ll}^{\delta}\right) = 0. \quad (7)$$

We now proceed as if the linear decomposition $\sigma = \sigma^{\psi} + \sigma^{\delta}$ holds everywhere, including near dislocation cores as defined by ψ. However, the computed stress field σ will be divergence free only away from any defect core. Given this decomposition $\sigma_{ij}^{\delta} = \epsilon_{ik}\epsilon_{jl}\partial_{ij}\chi - \sigma_{ij}^{\psi}$, we find an analogous result to Eq. (6),

$$(1-\kappa)\nabla^4\chi = \left(\epsilon_{ik}\epsilon_{jl}\partial_{ij}\sigma_{kl}^{\psi} - \kappa\nabla^2\sigma_{kk}^{\psi}\right). \quad (8)$$

Note that the stress σ^{ψ} from Eq. (3) is smooth and bounded, so the right-hand side of Eq. (8) can only give a nonsingular approximation to the singular right hand side of Eq. (6). Figure 1(c) shows the right-hand side of Eq. (8) obtained numerically for the dislocation dipole which is in good agreement with Eq. (6) obtained through demodulation (Fig. 1(d)). Notice that both methods act as regularizations of the singular density at defect cores.

From a given $\psi(\mathbf{r}, t)$ at time t, we compute σ^{ψ} from Eq. (3), and then solve Eq. (8) to obtain χ and therefore σ. The difference $\sigma_{ij}^{\delta} = \epsilon_{ik}\epsilon_{jl}\partial_{ij}\chi - \sigma_{ij}^{\delta}$ leads to the smooth strain $u_{ij}^{\delta} = (\sigma_{ij}^{\delta} - \nu\sigma_{kk}^{\delta}\delta_{ij})/(2\mu)$ which is, by construction, compatible. It can, therefore, be integrated to obtain a compatible deformation $\mathbf{u}^{\delta}$. The final step in the computation is to redefine the PFC density as $\psi'(\mathbf{r} + \mathbf{u}^{\delta}, t) = \psi(\mathbf{r}, t)$.

Although the stress-strain relation and stress superposition only hold far from defect cores, we define the stress of this newly deformed configuration everywhere as

$$\sigma_{ij} = \sigma_{ij}^{\psi} + \sigma_{ij}^{\delta} = \sigma_{ij}^{\psi} + \lambda\delta_{ij}u_{kk}^{\delta} + 2\mu u_{ij}^{\delta}, \quad (9)$$

which satisfies $\partial_j\sigma_{ij} = 0$ only far from defect cores. This is not a problem because standard diffusive evolution of the phase field suffices to equilibrate the stress near cores in time. We discuss this further below, and in Fig. 2.

The integration of u_{ij}^{δ} to obtain $\mathbf{u}^{\delta}$ is carried out through a Helmholtz decomposition into curl-free and divergence-free parts $u_i^{\delta} = \partial_i V + \epsilon_{ij}\partial_j A$. Applying the divergence to this expression, one obtains a Poisson equation for the potential V, $\partial_i u_i^{\delta} = u_{ii}^{\delta} = \nabla^2 V$, which is easily solved by spectral methods. On the other hand, taking the curl we find $\epsilon_{ij}\partial_i u_j^{\delta} = \epsilon_{ij}\epsilon_{jk}\partial_{ik}A = -\nabla^2 A$, which is a Poisson equation for A. Unfortunately the source term depends on the antisymmetric part of the smooth deformation gradient, which we do not obtain directly from the elastic stress, as this only depends on the symmetric part. We therefore apply another Laplacian operator to the equation, and use the compatibility relation $\epsilon_{ij}\partial_{ij}u_k^{\delta} = 0$ to find

$$\nabla^4 A = -\epsilon_{ij}\partial_{ik}(\partial_k u_j^{\delta} + \partial_j u_k^{\delta}) = -2\epsilon_{ij}\partial_{ik}u_{jk}^{\delta}. \quad (10)$$

This is a biharmonic equation for A with a known source term, which is again easily solved by spectral methods. In particular, if k_i are the components of the $\mathbf{k}$ vector and $\hat{u}_{ij}^{\delta}$ are the Fourier components of the residual strain, the
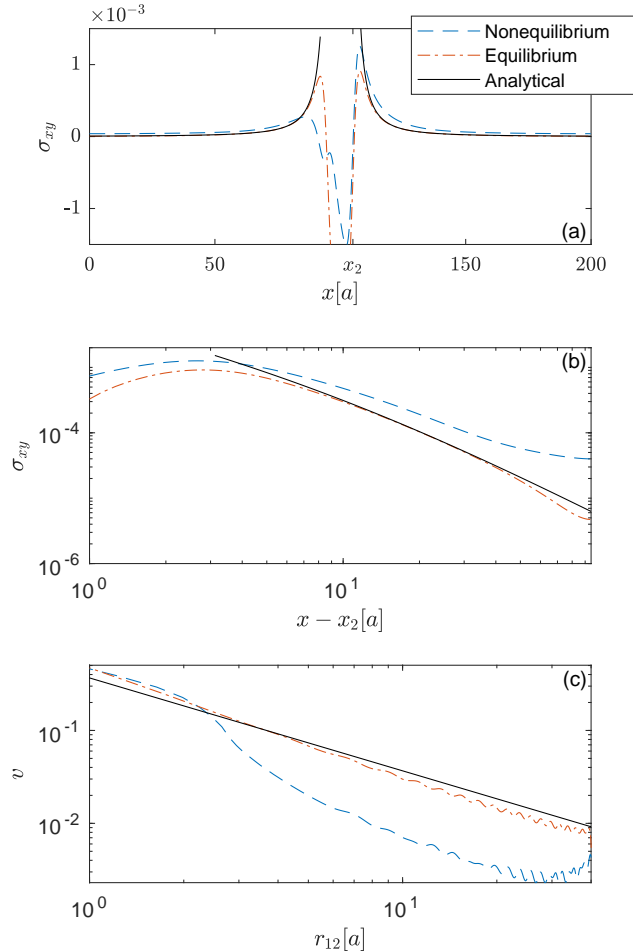
FIG. 2: (a) Shear stress σ_{xy}^{ψ} along the horizontal centerline of the rightmost dislocation core from direct integration of Eq. (2) (dashed line) compared with the our model (dot-dashed line) and Eq. (12) (solid line). (b) Shear stress as a function of the distance from the rightmost dislocation located at x_2 (marked in a), showing that the equilibrated stress follows linear elasticity from Eq. (12) in the far-field. (c) Dislocation velocity as a function of dipole separation $r_{12} = |\mathbf{r}_1 - \mathbf{r}_2|$ in the two models. Velocities are obtained from locating the zeros of the complex amplitudes of ψ as described in Ref. [25]. The Peach-Koehler force with stress given by Eq. (12), and mobility computed from $\mathcal{F}$ as given in [25]. There are no adjustable parameters in this calculation.

Fourier components of the residual deformation can be expressed as

$$\hat{u}_i^{\delta} = -\frac{ik_i}{k^2}\hat{u}_{jj}^{\delta} + 2i\epsilon_{ij}\epsilon_{rs}\frac{k_j k_r k_l}{k^4}\hat{u}_{sl}^{\delta}, \tag{11}$$

with the $k = 0$ component chosen to be zero to avoid rigid body displacements. We then compute the distorted PFC density $\psi'(\mathbf{r}) = \psi(\mathbf{r} - \mathbf{u}^{\delta})$ on the original grid $\mathbf{r}$ by expanding in Taylor series up to 5th in $\mathbf{u}^{\delta}$.

Next, we discuss a benchmark configuration: the relative motion of two edge dislocations along the same glide plane, Fig. 1(a). The periodic computational domain has 200×200 unit cells with a spatial resolution of $a/7 = 4\pi/7\sqrt{3}$ in the x direction, and $2\pi/6$ in the y direction. The initial distance between dislocations is $40a$, and we consider the parameters $r = -0.2, \psi_0 = 0.265$. We prepare the initial condition of $\psi(\mathbf{r}, t = 0)$ in the one-mode approximation and seeded with a dislocation dipole [25], and construct the distorted PFC density $\psi'(\mathbf{r}, 0) = \psi(\mathbf{r} - \mathbf{u}^{\delta}, 0)$ using Taylor expansion. We then solve Eq. (2) using an exponential-time differencing method with a time step of $\Delta t = 0.1$ [44]. For the PFC dynamics with mechanical equilibrium, we compute the distorted PFC density between each time steps. In the purely diffusive PFC, dislocations drift away from the center line in the climb direction before approaching each other to annihilate. This is suppressed under elastic equilibrium. Figures (2)(a,b) shows σ^{ψ} along a line going through the rightmost dislocation located at $\mathbf{r}_2$ at time $t = 3600$ obtained by direct integration of Eq. (2). This is compared to our model at $t = 779$, corresponding to a similar dipole size. In linear elasticity theory for an infinite, isotropic medium, the shear stress of a dipole is

$$\sigma_{xy} = \frac{2\mu(\lambda + \mu)}{\lambda + 2\mu} \sum_n \frac{b_x^n}{2\pi} \frac{\cos\phi_n \cos(2\phi_n)}{|\mathbf{r} - \mathbf{r}_n|}, \tag{12}$$

where ϕ_n is the azimuth relative to dislocation n, and we also compare with this expression. Divergences in Eq. (12) are regularized by ψ, and the stress near the cores is relatively well described by σ^{ψ} irrespective of whether the smooth distortion (11) is applied between time steps. Far from the cores, however, the two stresses show qualitatively different asymptotic dependence. The dot-dashed lines in Fig. (2)(a,b) show the stress in a configuration in which the smooth distortion (11) has been applied between time steps. The stress is still regularized near defect cores, yet agrees with linear elasticity in the far-field. Figure 2(c) shows the dependence of the dislocation velocity on the dipole separation as given by direct integration of Eq. (2), and by our model with imposed elastic equilibrium. For reference, we also show the expected result from linear elasticity by using the Peach-Koehler force with stress (12), and mobility derived from $\mathcal{F}$ (Eq. (45) in Ref. [25]). There are no adjustable parameters in the calculation of the analytic velocity. The two dislocations move towards each other until they annihilate, with a velocity inversely proportional to their separation. Our model captures this result well, while the direct integration approach shows significant qualitative deviation form the expected behavior.

To summarize, we have argued that the PFC model lacks deformation as an independent variable, and as a consequence fails to maintain proper mechanical equilibrium during plastic motion. We retain the model because it provides for lattice and topological defect structures

as derived properties from the phenomenological free energy. It also allows regularization of defect cores and singular stresses. PFC dynamics is also consistent with the classical Peach-Koehler force, with mobility that is again specified by the free energy $\mathcal{F}$. We take the view, however, that the PFC is not adequate to describe the distortion of the lattice away from moving defect cores, and hence supplement it with a smooth distortion field, compatible with the topological content of the ψ, but defined so as to maintain mechanical equilibrium everywhere away from defect cores. When the evolution of $\psi(\mathbf{r}, t)$ is thus constrained, we show numerically that our model agrees with the classical law of glide for a dislocation dipole in isotropic, linear elasticity. Dislocation climb is also captured by the diffusive PFC dynamics, and the elastic equilibrium constraint is the same as for glide. It would be interesting to further explore the effect of compressive stresses on dislocation climb. Although the analysis presented is based on a 2D triangular lattice, it can be generalized to other crystal lattices and 3D by modifying the symmetry of $\mathcal{F}$ [45], and by solving the corresponding anisotropic elasticity problem. These results put the PFC model on firmer ground to study more complex defected configurations at the nano- and mesoscale.

---

[1] J. Weiss and D. Marsan, Science **299**, 89 (2003).
[2] M. Koslowski, R. LeSar, and R. Thomson, Phys. Rev. Lett. **93**, 125502 (2004).
[3] F. F. Csikor, C. Motz, D. Weygand, M. Zaiser, and S. Zapperi, Science **318**, 251 (2007).
[4] P. D. Ispánovity, I. Groma, G. Györgyi, F. F. Csikor, and D. Weygand, Phys. Rev. Lett. **105**, 085503 (2010).
[5] P. D. Ispánovity, L. Laurson, M. Zaiser, I. Groma, S. Zapperi, and M. J. Alava, Phys. Rev. Lett. **112**, 235501 (2014).
[6] J. M. Tarp, L. Angheluta, J. Mathiesen, and N. Goldenfeld, Phys. Rev. Lett. **113**, 265503 (2014).
[7] Y. Cui, G. Po, and N. Ghoniem, Phys. Rev. Lett. **117**, 155502 (2016).
[8] A. Acharya, J. Mech. Phys. Solids **49**, 761 (2001).
[9] K. R. Elder, M. Katakowski, M. Haataja, and M. Grant, Phys. Rev. Lett. **88**, 245701 (2002).
[10] M. Haataja, J. Müller, A. D. Rutenberg, and M. Grant, Phys. Rev. B **65**, 165414 (2002).
[11] M. Koslowski, A. M. Cuitino, and M. Ortiz, J. Mech. Phys. Solids **50**, 2597 (2002).
[12] K. R. Elder and M. Grant, Phys. Rev. E **70**, 051605 (2004).
[13] S. Limkumnerd and J. P. Sethna, Phys. Rev. Lett. **96**, 095503 (2006).
[14] K. R. Elder, N. Provatas, J. Berry, P. Stefanovic, and M. Grant, Phys. Rev. B **75**, 064107 (2007).
[15] A. Acharya and C. Fressengeas, Int. J. of fracture **174**, 87 (2012).
[16] A. Acharya and C. Fressengeas, in *Differential Geometry and Continuum Mechanics* (Springer, New York, 2015).
[17] I. Groma, Z. Vandrus, and P. D. Ispánovity, Phys. Rev. Lett. **114**, 015503 (2015).
[18] A. D. Rollett, R. Suter, and J. Almer, Annu. Rev. Mater. Research **47** (2017).
[19] R. Suter, Science **356**, 704 (2017).
[20] A. Yau, W. Cha, M. Kanan, G. Stephenson, and A. Ulvestad, Science **356**, 739 (2017).
[21] J. P. Sethna, M. K. Bierbaum, K. A. Dahmen, C. P. Goodrich, J. R. Greer, L. X. Hayden, J. P. Kent-Dobias, E. D. Lee, D. B. Liarte, X. Ni, *et al.*, Annual Review of Materials Research **47**, 217 (2017).
[22] H. Emmerich, H. Lwen, R. Wittkowski, T. Gruhn, G. I. Tth, G. Tegze, and L. Grnsy, Advances in Physics **61**, 665 (2012).
[23] P. Stefanovic, M. Haataja, and N. Provatas, Phys. Rev. Lett. **96**, 225504 (2006).
[24] P. Y. Chan, G. Tsekenis, J. Dantzig, K. A. Dahmen, and N. Goldenfeld, Physical review letters **105**, 015502 (2010).
[25] A. Skaugen, L. Angheluta, and J. Viñals, Phys. Rev. B **97**, 054113 (2018).
[26] V. Heinonen, C. V. Achim, K. R. Elder, S. Buyukdagli, and T. Ala-Nissila, Phys. Rev. E **89**, 032411 (2014).
[27] V. Heinonen, C. V. Achim, J. M. Kosterlitz, S.-C. Ying, J. Lowengrub, and T. Ala-Nissila, Phys. Rev. Lett. **116**, 024303 (2016).
[28] A. M. Kosevich, in *Dislocations in Solids*, Vol. 1, edited by F. R. N. Nabarro (North-Holland, New York, 1979) p. 33.
[29] D. R. Nelson and J. Toner, Phys. Rev. B **24**, 363 (1981).
[30] J. M. Rickman and J. Viñals, Phil. Mag. A **75**, 1251 (1997).
[31] K. Aguenaou, *Modeling of solidification*, Ph.D. thesis, McGill University (1997).
[32] A. Acharya, J. Mech. Phys. Solids **52**, 301 (2004).
[33] J. Berry, M. Grant, and K. R. Elder, Phys. Rev. E **73**, 031609 (2006).
[34] S. van Teeffelen, R. Backofen, A. Voigt, and H. Löwen, Phys. Rev. E **79**, 051404 (2009).
[35] E. D. Siggia and A. Zippelius, Phys. Rev. A **24**, 1036 (1981).
[36] G. Tesauro and M. C. Cross, Phil. Mag. A **56**, 703 (1987).
[37] A. Adland, Y. Xu, and A. Karma, Phys. Rev. Lett. **110**, 265504 (2013).
[38] D. Taha, S. K. Mkhonta, K. R. Elder, and Z.-F. Huang, Phys. Rev. Lett. **118**, 255501 (2017).
[39] E. J. Schwalbach, J. A. Warren, K.-A. Wu, and P. W. Voorhees, Phys. Rev. E **88**, 023306 (2013).
[40] Z.-F. Huang and K. R. Elder, Phys. Rev. Lett. **101**, 158701 (2008).
[41] D. Boyer and J. Viñals, Phys. Rev. Lett. **89**, 055501 (2002).
[42] B. Perreault, J. Viñals, and J. M. Rickman, Phys. Rev. B **93**, 014107 (2016).
[43] M. C. Cross and D. I. Meiron, Phys. Rev. Lett. **75**, 2152 (1995).
[44] S. M. Cox and P. C. Matthews, Journal of Computational Physics **176**, 430 (2002).
[45] M. Greenwood, N. Provatas, and J. Rottler, Phys. Rev. Lett. **105**, 045702 (2010).